Real Time SAXS/Stress-Strain Studies of Thermoplastic Polyurethane - A fibre diffraction approach to a non-crystalline material

D J Blundell[1], C Martin[1], A Mahendrasingam[1], W Fuller[1] and G Eeckhaut[2]

1. Dept of Physics, Keele University, Staffordshire ST5 5BG, UK

2. Huntsman Polyurethanes, Everslaan 45, B-3078 Everberg, Belgium

Received November 2001; accepted in revised form 14th March 2002.

Introduction

Elastomeric polyurethanes are synthesised from blocks of flexible, "soft" units linked together with rigid, "hard" blocks. Incompatibility between hard and soft blocks leads to phase separation giving rise to two-phase morphologies with an approximate 10nm spatial correlation which can be monitored by SAXS.

Despite their versatility for a wide range of uses, applications of polyurethanes are still limited by their relatively high mechanical hysteresis compared with other elastomers. This hysteresis and the associated mechanical loss processes can be partly attributed to the breakdown and reformation of the phase structure during mechanical cycling.

This paper focuses on one aspect of an on-going programme between Keele University and Huntsman Polyurethanes. It involves simultaneously measuring the SAXS patterns and the stress during tensile deformation in order to follow the changes in morphology and identify effects associated with mechanical loss.

It is currently believed that phase separation (on cooling or during solvent evaporation) generally occurs via spinodal decomposition followed by ripening [1-3]. The exact nature of the final morphology is uncertain and depends on the fabrication route and on the molecular formulation. Several approaches are being used to elucidate the nature of both the starting morphologies and how the morphologies change during deformation. This paper describes a novel approach to the analysis of two dimensional SAXS patterns and is illustrated with recent results from one particular polyurethane. The analysis is based on an affine deformation scheme in which some of the ideas are borrowed from fibre diffraction crystallography.

Experimental Results

The particular polyurethane used in this study had a soft segment derived from an a,w dihydroxy poly(tetrahydrofurane) of molecular weight 1000. The hard segments consisted of mixtures of toluene diisocyanate, 4,4' -methylene phenylene diisocyanate and ethanolamine in a molar ratio = 2/1/2. The volume fraction of the hard segments in the final polyurethane was approximately 0.36.

Specimens in the form of 0.5mm thick sheets were deformed in a purpose built stretching camera [4] mounted on beamline 16.1 at the SRS in Daresbury using the Fast 2D detector to monitor the SAXS. The specimen was subjected to a continuous cycle of extensions and retractions. Figure 1 shows the variation in tensile force during the cycle in which the SAXS patterns were recorded with sequential 3.2 second frames. Figure 2 shows the same force data plotted against draw ratio and illustrates the hysteresis effect during the cycled oscillations. The draw ratios in these experiments have been derived from grating markings on the sample using a video image that had been recorded simultaneously with the force and SAXS patterns. It will be noted that the shape of the force variation during the first extension indicates a mechanical yield process followed by a more linear response at around the point corresponding to frame 10 where the draw ratio is about 1.25. Selected SAXS frames from this

50

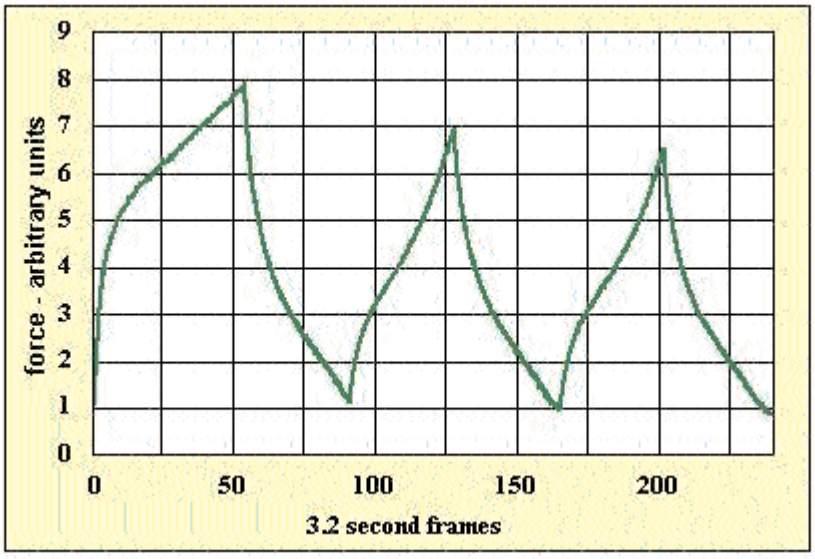

Figure 1: Variation in tensile force during extension and retraction cycle.

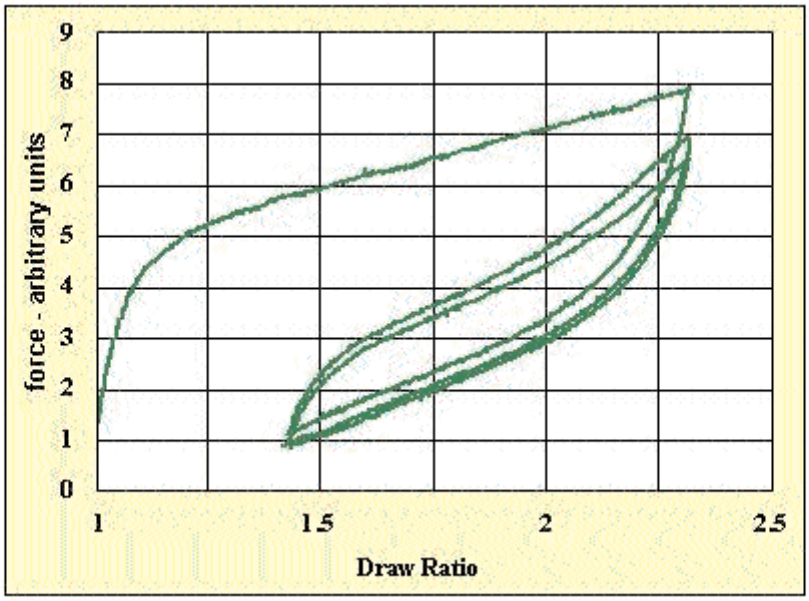

Figure 2: Tensile force plotted against draw ratio showing hysteresis effect.

experiment during the first tensile extension are illustrated in Figure 3.

The initial SAXS pattern from the undeformed sample in frame 1 is an isotropic halo with a peak intensity equivalent to a Bragg periodicity of 10.4nm. During the first tensile extension, the diffraction halo intensifies on the meridian and becomes progressively elliptical in shape. Confirmation that the halo maximum follows the locus of an ellipse (ie. $x^2/a^2 + z^2/b^2 = 1$) can be seen from plots of x^2 vs z^2 as in the examples in Figure 4, where z is in the vertical draw direction and x is in the lateral direction. This paper is primarily concerned with describing an analytical method for interpreting the shape and intensity distribution of these elliptical patterns during this first tensile extension. Further papers will address the ramifications of this interpretation in more detail and will also deal with the subsequent changes in the patterns during retraction.

Affine Deformation

An elliptical locus can be derived from a circle by an affine deformation; ie a deformation in which all x and y coordinates are systematically multiplied by constants fx and fy respectively. It is therefore of interest to enquire whether the elliptical halo is directly linked with an affine deformation of the two phase structure in the specimen. To a good approximation, polyurethane elastomers deform at constant volume. Thus during uniaxial tensile deformation of draw ratio λ, the length of the sample will change by λ while the lateral dimensions will change by a factor of $1/\sqrt{\lambda}$. If the two phase

51

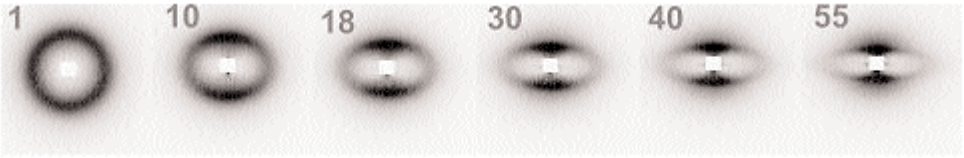

Figure 3: Selected SAXS patterns for frames 1, 10, 18, 30, 40 and 55 during the first extension of the deformation cycle.

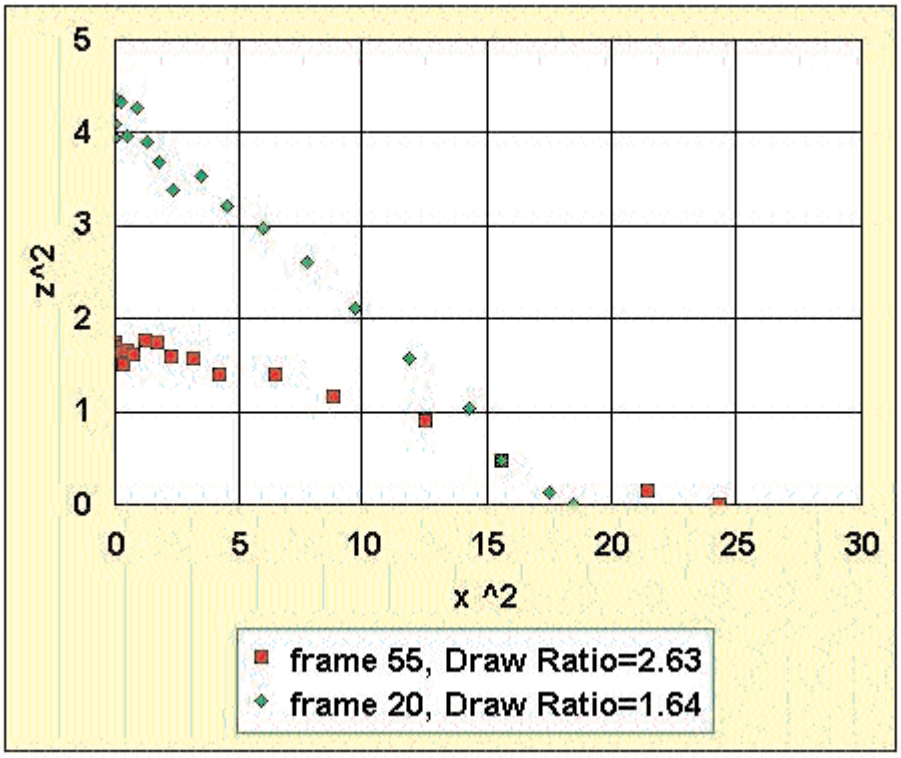

Figure 4: Example plots of loci of intensity maxima around the elliptical pattern for frames 20 and 55.

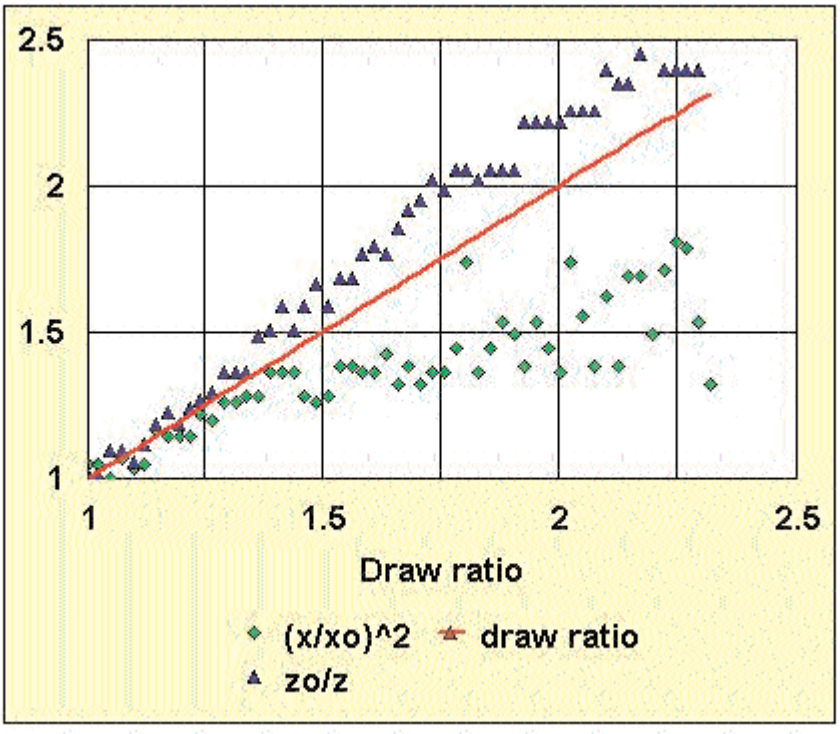

Figure 5: Plots of z_o/z and x^2/x_o^2 versus draw ratio, showing agreement with affine deformation scheme up to $l \sim 1.25$.

microstructure follows an affine deformation scheme related to the overall sample shape then the x and z coordinates of a vector between any two structural elements in real space will be modified by the same factors. In such a situation, the corresponding intensity function in reciprocal space will also deform affinely but with factors that are the inverse of those in real space. Thus x and z coordinates of vectors in reciprocal space will be changed by factors of $1/\lambda$ and $\sqrt{\lambda}$ respectively. If the circular halo of the undeformed specimen has a radius x_o $(=z_o)$ then $x/x_o = \sqrt{\lambda}$ and $z/z_o = 1/\lambda$. This hypothetical situation can be partially tested on the experimental data by plotting the two parameters $(x/x_o)^2$ and z_o/z versus l as in figure 5. The data points closely follow the value of λ up to a draw ratio of around 1.25. Beyond this the data points diverge and indicate a larger degree of ellipticity than that predicted for affine deformation. The point of the divergence corresponds to the onset of the more linear response in Figures 2 and 3 and suggests there may be a link with the way in which the microstructure deforms.

Up until this point there is therefore an indication that the main features of the microstructure are deforming in a way that is related to an affine scheme. One needs to examine the implications of this for the nature of the phase morphology. In a true affine deformation, every feature and shape of the phase morphology would need to deform in an affine manner. In an associated way all the features of the corresponding intensity function in reciprocal space would undergo a reciprocal affine deformation. Thus a circular diffraction halo with uniform intensity would deform to an oblate ellipse that also had a uniform intensity. However the observed elliptical halos in figure 3 up to frame 10 do not have a uniform intensity but exhibit an intensification on the meridian. One can conclude therefore that, despite the ellipticity being consistent with affine deformation, the shapes of the microphases are not themsleves following the true affine scheme.

Statistical Particulate Model

The above conclusion is not surprising if one bears in mind the composition of the polyurethane elastomer. It is unrealistic to expect the above true affine model to hold since the hard and soft phases have quite different mechanical properties. The hard microphase regions will resist changes in shape while the soft phase will tend to change shape to accommodate the hard phase. When the hard phase is in the minority, as in this specimen, the degree of connectivity of the hard phase will be reduced. One would therefore expect that the larger concentrations of hard phase will be more able to retain their original shapes during the deformation of the macroscopic sample. It is therefore of interest to consider a modified affine model in which the hard microphase regions can effectively be represented by separated particulate inclusions embedded in a continuous soft phase and to ignore any minor

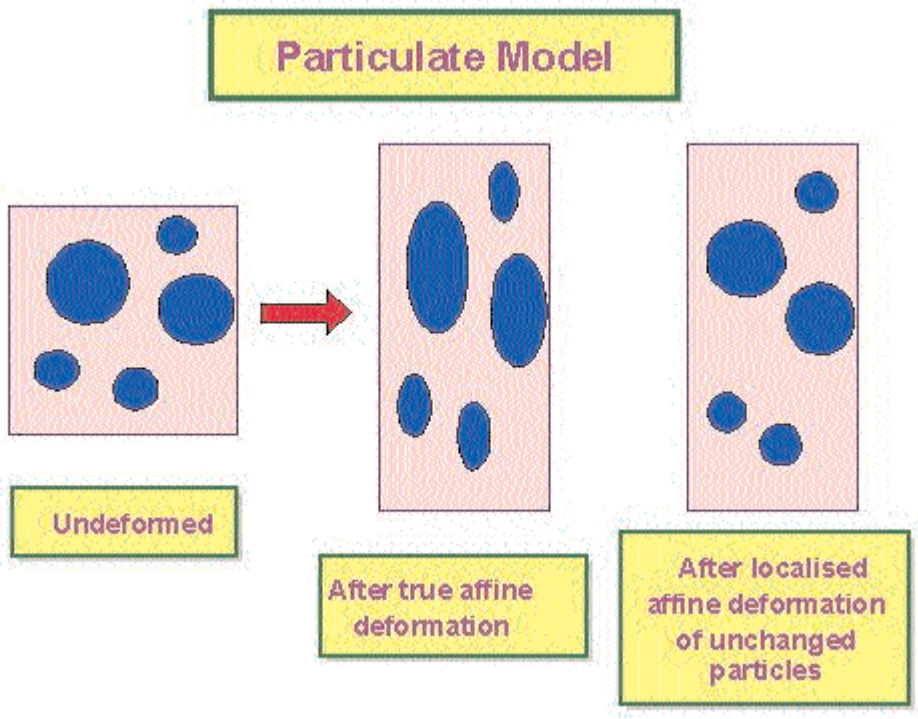

Figure 6: Illustration of particulate model showing differences between pure affine deformation and modified affine deformation.

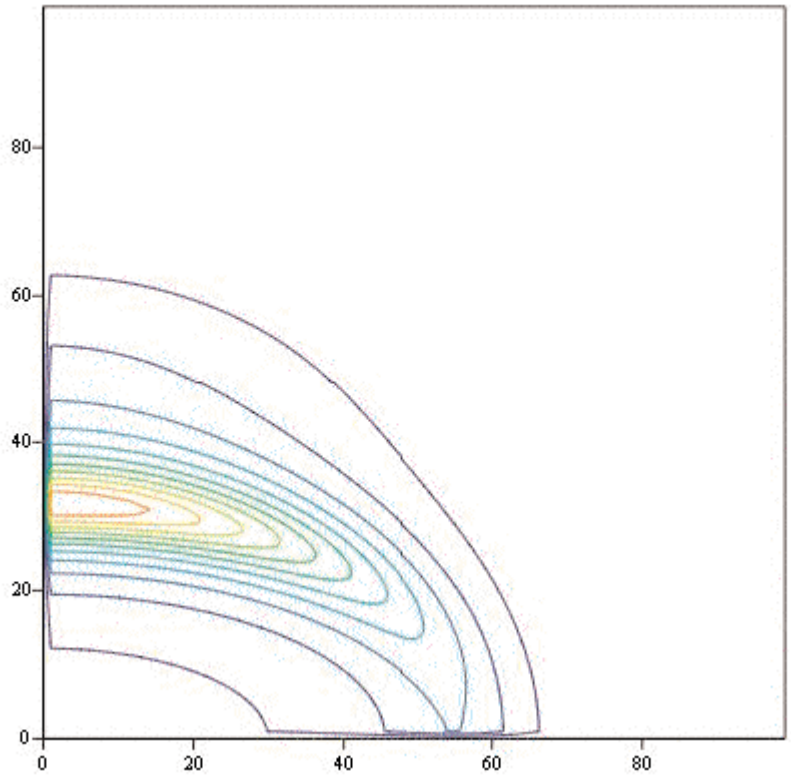

Figure 7: Predicted SAXS pattern for a model example of spherical particles on a deformed statistical lattice.

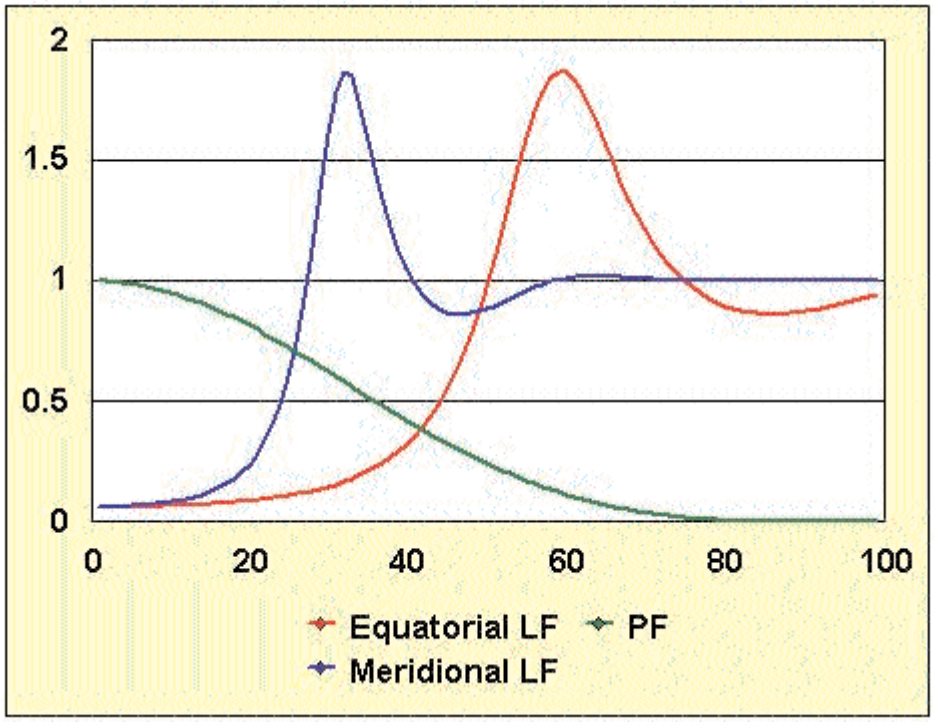

Figure 8: Contributions of LF and PF factors for predicted pattern in figure 7.

regions of connectivity. Assume therefore that during deformation, the relative positions of the hard phase particles with respect to each other move affinely but the shapes of the particles remain unchanged. In this model the particles represent the main concentrations of hard phase and will vary in shape and size. The contrast between true affine and the modified affine deformation is shown in Figure 6 for the simplified case of spherical particles.

The diffraction halo will result from the interference between waves scattered from this statistical arrangement of particles. Making the analogy with standard crystallography, one can consider the particles to be located on statistical lattice points. The observed intensity along any given scattering direction will therefore be the product of a Particle Function (*PF*) and a Lattice Function (*LF*). In the

undeformed, isotropic state, *LF* will be centrosymmetric. During deformation the statistical lattice points will move according to the affine scheme. The *LF* will then vary with direction in such a way that the profile of *LF* will deform in an affine manner that is the reciprocal of the deformation of the statistical lattice. In contrast, *PF* will be isotropic and will remain unchanged during deformation. Accordingly the peak intensity of the observed intensity halo in any particular direction will be determined by the value of *PF* at the peak scattering vector. This is analogous to the crystallography of perfect crystals where the intensity of each discrete crystalline reflection is due to the sampling of the structure factor of the unit cell at each reciprocal lattice point. As an illustrative example of a statistical lattice consider the simple case in which the periodic regularity in any particular direction is represented by a one dimensional lattice factor (*LF*) in the form of a Zernike-Prins term.

$$LF = \frac{(1-|F|^2)}{(1-2.|F|.\cos(qd)+|F|^2)}$$

where

$$F = \exp(\frac{-\pi^2 q^2 g^2 d^2}{2})$$

and d is the periodic repeat and g is the fractional deviation of the distribution of projected distances between scatterers.

Also for simplicity, assume that the hard phase inclusions can be represented by identical spheres of radius R with a particle scattering factor,

$$PF = \frac{9.(\sin(Rq) - R.q.\cos(Rq))^2}{(R.q)^6}$$

The predicted intensity is the product of the two terms. During deformation, the periodic distance *d* will vary with direction according to an affine scheme causing the *q*-radius at the peak of the halo to vary with direction in a reciprocal way. The intensity around the halo will be determined by the value of *PF* at each peak *q*. Figure 7 shows one quadrant of a predicted SAXS pattern expected for an affine deformed sample for the particular case where:-

the sphere radius is 0.4 of the average periodic repeat,
the deviation g is 0.25 of the periodic repeat and the draw ratio λ = 1.4.

Figure 8 illustrates how the *LF* and *PF* contribute to the intensity of the elliptical halo along the meridan and equator axes.

Figure 7 reasonably reproduces the features of the observed SAXS patterns. If one accepts this approach for interpreting the experimental patterns

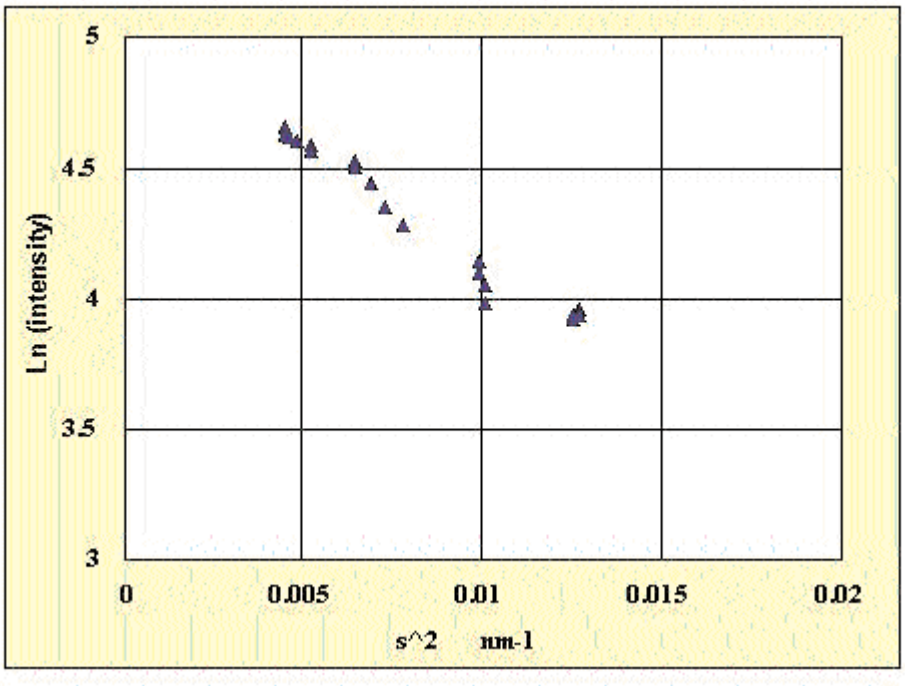

Figure 9: Variation of peak intensity around ellipse for frame15, plotted in the form of a Guinier Plot.

then one can consider the corollary of the argument that the intensity variation around the ellipse gives direct information of the structure factor of the particles located on the statistical lattice. (Interestingly, the exact form of the Lattice Factor does not need to be known providing the positions of the statistical lattice points deform affinely.) Figure 9 shows the variation of intensity as a function of the square of the radii for frame 10, plotted on a log scale. This is equivalent to a Guinier plot for the scattering particles [5] plotted between the limits of the major and minor axes of the elliptical halo. A linear fit to these points indicates that the effective radius of gyration of the particles is 2.7 nm. Identical spherical particles with this radius of gyration would have a diameter of 6.9 nm. Bearing in mind the dispersity in size expected for the equivalent particles that represent the hard phase concentrations in this model, this derived particle dimension is sensibly consistent with the 10.4 nm periodic repeat of the undeformed diffraction halo.

Implications of Affine Model

This analytical approach implies that the hard phase in this particular specimen tends to concentrate into regions that can be approximated to particles and that during the first part of deformation these effective particles separate from each other in an affine manner. Since the phase separation is expected to be initiated via a spinodal decomposition there is expected to be a degree of interconnectivity in the final ripened morphology. The analysis implies that any such connections do not significantly impair the movement of the main hard phase concentration during the initial deformation. It is of interest to note that the additional insight into the nature and size of the hard phase concentrations which is provided by this approach is obtained independently of a direct analysis of the SAXS pattern of the undeformed sample.

It should be noted that there is considerable variation in the formulation of thermoplastic polyurethanes and that other specimens have been observed in which the development of the SAXS patterns differs from the present example and where the above affine deformation approach would therefore not be applicable.

References

[1] Ryan, A.J., Willkomm, W.R., Bergstrom, T.B., Macosko, C.W., Koberstein, J.T., Yu, C.C. and Russell, T.P., *Macromolecules* (1991) 24, 2883.

[2] Elwell, M.J., Mortimer, S. and Ryan, A.J., *Macromolecules* (1994) 27, 5428.

[3] Ryan, A.J., Macosco, C.W. and Bras, W., *Macromolecules* (1992) 25, 6277.

[4] Mahendrasingam, A, Fuller, W., Forsyth, V.T., Oldman, R.J., Mackerron, D.H. and Blundell, D.J., *Rev. Scientific Instruments* (1992) 63, 1087.

[5] Guinier, A., X-ray Diffraction in Crystals, *Imperfect Crystals and Amorphous Bodies*, (W.H.Freeman, San Fransisco, 1963)